

A compact gamma-ray detector using wavelength-shifting fibers coupled to YAP scintillation crystal

ZHU Jie^{1,2} MA Hongguang¹ MA Wenyan¹ ZENG Hui^{2,*} WANG Zhaomin² XU Zizhong²

¹ Department of Nuclear Engineering, The Second Artillery Engineering Institute, Xi'an 710025, China

² Department of Modern Physics, University of Science and Technology of China, Hefei 230026, China

Abstract The performance of a compact position sensitive gamma-ray detector based on wavelength-shifting fibers coupled to YAlO₃:Ce scintillation crystal was evaluated using a Monte-Carlo simulation method. The simulation model has been setup using the GEANT4 codes. Compared with the gamma-ray detector based on the YAlO₃:Ce scintillation crystal coupled to Hamamatsu R2486 position sensitive photomultiplier tube, the results indicate that the gamma-ray detector based on wavelength-shifting fibers readout has good position linearity, good spatial resolution and larger effective field of view. The image and point spread function of measured point were presented. The spatial resolution response as a function of position was obtained. The factors influencing spatial resolution and position linearity were discussed.

Key words Monte-Carlo simulation, WSF, Spatial resolution

CLC numbers TL812, R730.44

1 Introduction

Gamma camera has been in wide use in nuclear medicine, and great efforts have been made in developing compact gamma camera with good spatial resolution^[1-3]. To achieve clear nuclear medical image, the gamma-ray detectors should be small and flexible with good spatial resolution. At present, a planar crystal coupled to position-sensitive photomultiplier tube (PSPMT^[4]) provides better spatial resolution than a gamma-ray detector of conventional Anger camera^[5]. However, the big light spread produced by planar crystal causes a distorted region (2~3 cm) around the PSPMT boundaries^[6]. So effective field of view of the camera is relatively small and the spatial resolution is only 4~5 mm. Also, gamma camera uses planar crystal coupled to PSPMT has relatively high cost per unit photocathode area.

In an attempt to address the issue, we have been

developing a γ -ray detector which detects the interactions position of γ -rays by measuring profiles of light trapped inside ribbons of wavelength-shifting fibers (WSFs) coupled to a planar crystal. The fibers are placed in orthogonal directions (X and Y) on each side of the crystal. A coincidence of signals from X and Y tells the position of γ -ray. The WSF readout improves the position resolution and decreases the required photocathode area of PSPMT. In other words, the same area of PSPMT can be used for larger image area. With this type of γ -ray detector, a gamma camera is compact, has larger effective field of view and costs less. In this paper, a simulation model for compact γ -ray detector with WSFs coupled to planar scintillation crystal is developed using the GEANT4 codes. The performance is assessed in terms of total number of photons, spatial resolution and position linearity.

Supported by National Natural Science Foundation of China (No.10275063)

* Corresponding author. E-mail address: zhui@ustc.edu.cn

Received date: 2007-10-29

2 Materials and description of the simulation

2.1 YAP and WSF

The $\text{YAlO}_3:\text{Ce}$ (YAP) scintillation crystal is used in γ -ray imaging systems with very high spatial and time resolution for applications in nuclear medicine^[7]. It has an emission spectrum peaking at 370 nm, scintillation decay time of 30 ns and light output of about 1.7×10^4 photons/MeV. The size of YAP scintillation crystal is $20\text{mm} \times 20\text{mm} \times 4\text{mm}$ in our simulation. The WSF is widely used in high-energy physics to concentrate light from large areas onto smaller photosensors. It absorbs short-wavelength incident photon and isotropically emits secondary longer-wavelength photons. The SCSF-38 WSFs^[8] have an absorption spectrum peaking at 390 nm and an emission spectrum peaking at 440 nm. Because the WSF absorption spectrum nearly overlaps the YAP emission spectrum, a majority of the light escaping from the YAP crystal is collected by the fibers. In our simulation, the SCSF-38 WSFs are $\Phi 2 \text{ mm} \times 300 \text{ mm}$, with refractive index of the WSFs and cladding being 1.59 and 1.49, respectively, and the surrounding medium is silicone gel.

2.2 The light transmission efficiency

An incident photon interacts with the YAP crystal and produces scintillation light. The light produced by each interaction event travels inside the crystal toward the surface. The light transport is an exponential attenuation process, which takes into account both multiples reflections and self-absorption. The amount of light escaping from the crystal surface can be calculated as the fraction of solid angle defined by the limit angle between YAP (with refractive index of 1.94) and silicone gel (with refractive index of 1.40). It is about 85%. Not all the light escaping from the crystal is collected by the fibers. At the YAP-silicone gel interface and silicone gel-fibers interface, the light transmission is about 93%, calculated with the Fresnel relations for normal incidence. The fiber absorption spectrum does not overlap the YAP emission spectrum perfectly. This produces an additional loss. About 84% of the light is absorbed by the fiber and re-emitted with a quantum efficiency of 80%^[9]. Only a fraction of

the re-emitted light are trapped inside the fiber and then piped to the fiber ends due to different refractive indexes of the fiber core and cladding. From a calculation using the refractive indexes, 18.5% of the light is trapped in the fiber. The light transport along the fiber can also be described as an exponential attenuation process. As the other end was aluminized to improve light collection at PSPMT, the total light escaping from the fiber end is 50%. The detector uses Hamamastu R2486 PSPMT, which has a quantum efficiency of 20% at 440 nm.

2.3 Description of the simulation

The simulation is based on the GEANT4 program library developed at CERN. The geometric description of simulative prototype is shown in Fig.1. Two ribbons of SCSF-38 WSFs are coupled with silicone gel to opposite sides of a YAP slab. As confirmed previously^[10], the number of photons is higher using silicone gel to couple the fibers to the crystal. Each ribbon contains 10 WSFs. The fiber ribbons are placed in orthogonal directions (X and Y) on each side of the crystal in order to provide position information on both directions. The top surface is X (WSF- X) and the bottom surface is Y (WSF- Y).

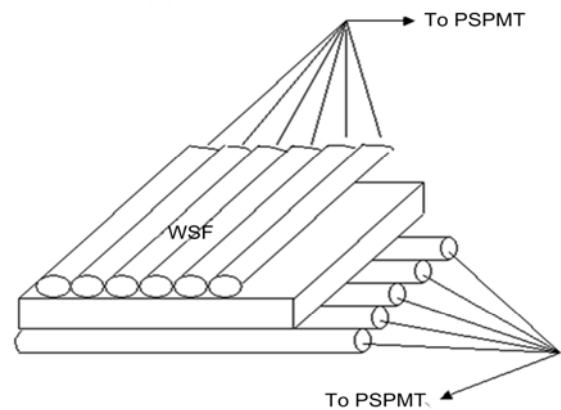


Fig.1 A schematic diagram of the simulative prototype.

With a beam of γ -rays incident on the crystal perpendicularly, the simulation is carried out as follows. (1) Tracing the i -th γ -ray event and marking the interaction coordinates. (2) Calculating energy deposit of the secondary electrons. (3) Converting the deposit energies to scintillation photons, which emit isotropically. (4) A fraction of the photons is absorbed

by the WSFs and is followed by isotropic emission. (5) Tracing the scintillation photons according to the Fresnel relations until scintillation photons hit the photocathode of PSPMT and converted to photoelectrons with quantum efficiency of 20%. (6) Recording the coordinate of photoelectrons (x_{ij} , y_{ij}) and the interaction coordinate of i -th gamma photon would be calculated with the following formula

$$X_i = \frac{\sum_{j=1}^{m_i} x_{ij}}{m_i}$$

$$Y_i = \frac{\sum_{j=1}^{m_i} y_{ij}}{m_i}$$

where m_i is the total count of the photoelectrons detected in the i -th γ -ray event. It is assumed that PSPMT is an ideal position sensitive component and its readout coordinates just correspond to (x_{ij} , y_{ij}).

3 Results and discussion

In order to evaluate performance of the position sensitive γ -ray detector based on WSF coupled to YAP scintillation crystal, we simulated with 10^5 events of 59.5 keV and 140 keV γ -rays hitting perpendicularly the surface of crystal on coordinates of (11 mm, 11 mm) respectively. The interaction position is located approximately above WSFs- X_6 and WSFs- Y_6 .

3.1 Total number of photons produced by WSFs

Fig.2 shows the total number of photons produced by WSFs on the coordinate of (11 mm, 11 mm). Fig.2a stands for 10^5 events of 59.5 keV γ -ray, while Fig.2b stands for 10^5 events of 140 keV γ -ray.

From Fig.2, one can find: (1) A large number of the photons is produced in the corresponding WSFs close to the beam of γ -rays. The photons trapped in the WSFs are sufficient to provide high probability of detection of the event. (2) Near the hitting point of γ -ray only a few WSFs contain position information. This improves spatial resolution of the γ -ray detector when the position of γ -ray interaction is estimated by a centroid calculation.

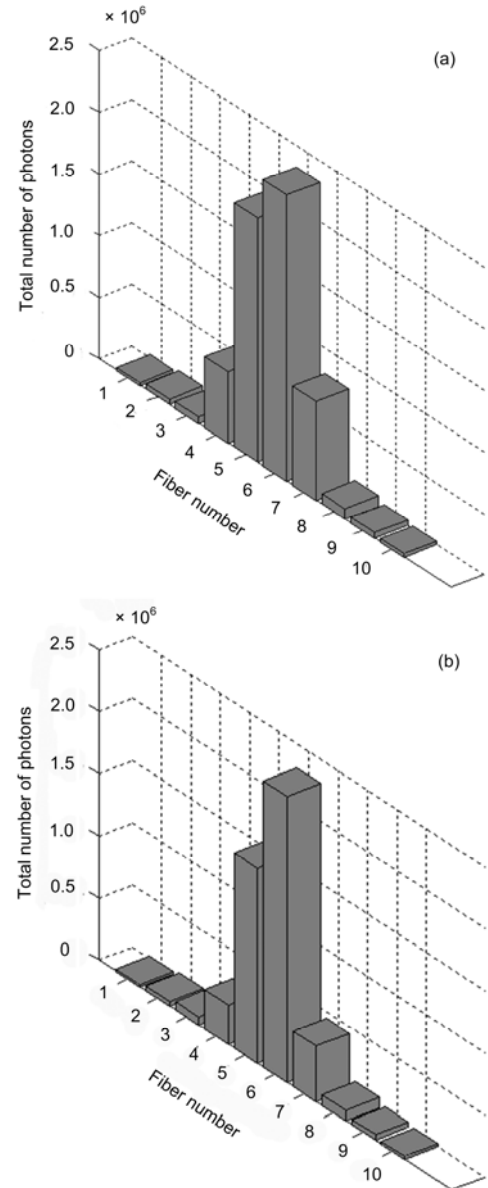


Fig.2 Total number of photons, produced by WSFs on the coordinate of (11mm, 11mm), of 59.5 keV (a) and 140 keV (b). The light distribution over the WSFs is narrower for the 140 keV γ -ray interactions.

3.2 Spatial resolution

Fig.3 shows the image obtained with 10^5 events of 140 keV γ -ray. The interaction position is located approximately above WSF- X_6 and WSF- Y_6 . Fig.4 shows the point spread function (PSF) of the measured point. By fitting a Gaussian curve to the PSF, a spatial resolution of 1.1 mm FWHM (full width at half minimum) is obtained for both x and y directions. To obtain the spatial resolution response as a function of position for the compact γ -ray detector based on WSF readout, the γ -ray scanned the YAP surface from 2 mm to 18 mm with a step of 2 mm along a diagonal of the

YAP crystal. Nine points were obtained. By using the same analysis process, spatial resolutions of all the irradiation spots were obtained. Fig.5 shows the spatial resolution response as a function of position for the γ -ray detector. Averaged at 1.21 mm FWHM, the best spatial resolution was 1.1 mm FWHM.

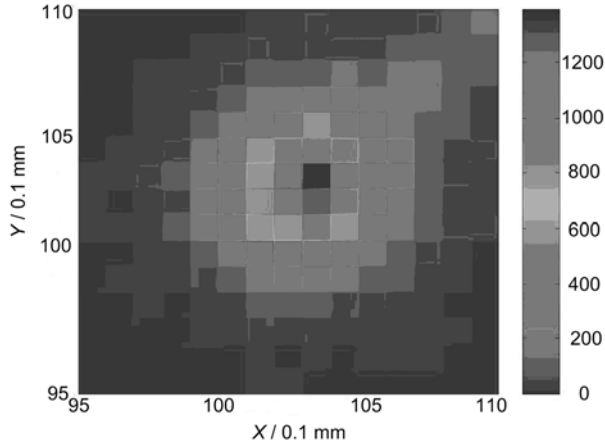


Fig.3 Image of the measured point.

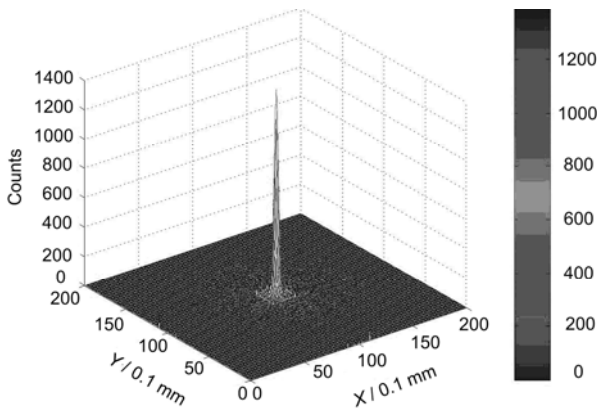


Fig.4 Point spread function of the measured point. A spatial resolution of 1.1 mm FWHM is obtained.

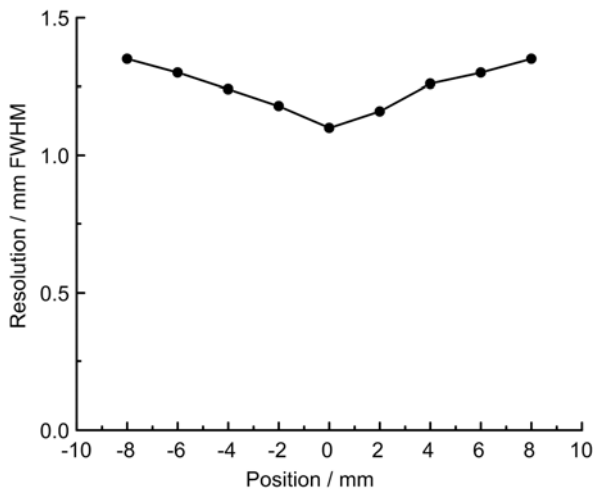


Fig.5 Spatial resolution response as a function of position for the γ -ray detector.

3.3 Position linearity

With the results of the nine measured points, the position linearity of the detector can be studied (Fig.6). The images of Point 1 and 9 were significantly distorted. This is due to the shrinkage effect near the edges of the crystal^[6]. And the light reflection on the boundaries of the crystal aggravated the shrinkage effect, hence the position distortions near the edges of the crystal. The light-reflection will be optimized with a variety of circumstances of boundaries.

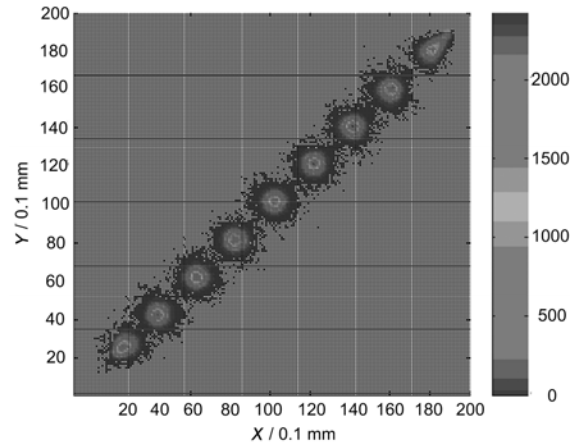


Fig.6 Images of the measured points and the two-dimensional position linearity.

The results show that position linearity in a range of 16 mm is good. So the effective field of view (FOV) is 80%. All the nine points can be separated from each other. This means that spatial resolution of the detector is less than 2 mm, which is in agreement with the simulation results. Except for Point 1 and 9, the images of the other points are of central symmetry. This demonstrates that the performance of the detector for γ -ray imaging is excellent.

A γ -ray detector based on the YAP scintillation crystal coupled to Hamamatsu R2486 position sensitive photomultiplier tube was built^[11]. To study the position linearity and effective field of view of the detector, the surface of YAP crystal was scanned by a collimated ²⁴¹Am source. The scan range was from -10 mm to +10 mm with a step of 1mm along one crystal axis. Data of 19 points were collected.

Fig.7 shows the position linearity response of the detector. The data fit with a straight line. The results show that position linearity in a range of 12 mm is good. So the effective field of view (FOV) is only 60%.

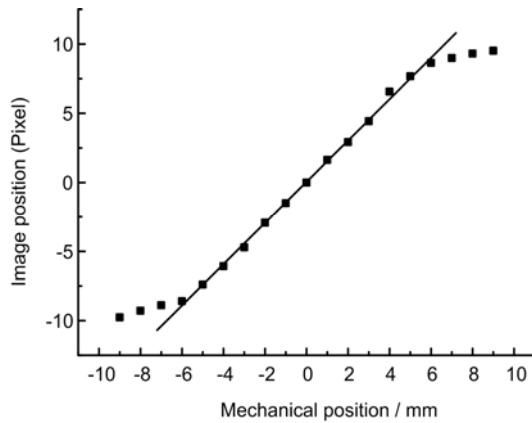


Fig.7 Position linearity response of the γ -ray detector based on YAP scintillation crystal coupled to Hamamastu R2486 PSPMT.

Fig.8 shows the spatial resolution response as a function of position for the detector. A mean value of spatial resolution of 5.7 mm FWHM and a best value of 4.3 mm FWHM were obtained. The deterioration of spatial resolution is evident.

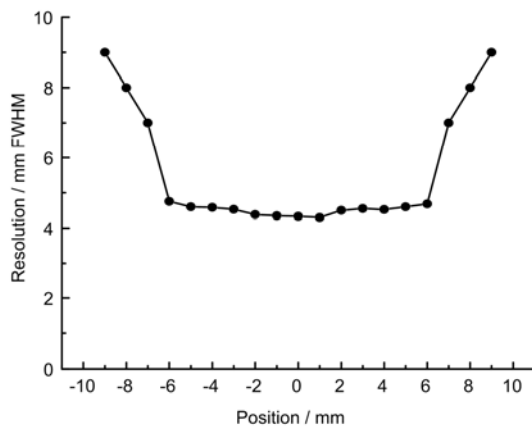


Fig.8 Spatial resolution response as a function of position for the γ -ray detector based on YAP scintillation crystal coupled to Hamamastu R2486 PSPMT.

Compared with γ -ray detectors based on the YAP scintillation crystal coupled to Hamamastu R2486 PSPMT, the results indicate that the γ -ray detector based on WSF readout has better position linearity and spatial resolution and larger effective field of view. Although it costs more, the γ -ray detector based on WSF readout is a promising candidate for nuclear medical imaging applications.

4 Conclusions

A compact position sensitive γ -ray detector using wavelength-shifting fibers coupled to a YAP planar scintillation crystal has been studied *via* Monte-Carlo simulations. Results demonstrate the feasibility of the

concept of the compact gamma-ray detector based on wavelength-shifting fibers readout. Monte-Carlo simulations indicate that such a gamma-ray detector can achieve very good performance for gamma-ray imaging. A mean value of spatial resolution of 1.21 mm FWHM and a best value of 1.1 mm FWHM were obtained. The effective field of view (FOV) is 80%. For the γ -ray detectors based on the YAP scintillation crystal coupled to Hamamastu R2486 PSPMT, a mean value of spatial resolution of 5.7mm FWHM and a best value of 4.3 mm FWHM were obtained, the effective field of view (FOV) was only 60%. The simulations also demonstrate that the light-reflection effects on the boundaries of the crystal aggravate the shrinkage effect and the position distortions near the edges of the crystal. A way of decreasing the shrinkage effect is by optimizing the light-reflection effects on the boundaries of the crystal. In the future Monte-Carlo simulations work, we will continue to work on such optimization with a variety of scintillators, wavelength-shifting fibers, and position sensitive photomultiplier tubes.

References

- 1 Bird A J, Ramsden D. Nucl Instrum Methods Phys Res A, 1990, **A299**: 480-483.
- 2 Majewski S, Farzanpay F, Goode A, *et al.* Nucl Instrum Methods Phys Res A, 1998, **A409**: 520-523.
- 3 Garibaldi F, Cisbani E, Cusanno F, *et al.* Nucl Instrum Methods Phys Res A, 2001, **A471**: 222-228.
- 4 Position sensitive photomultiplier tube with crossed wire anodes R2486 series, Specifications manual (in Japanese). Hamamatsu: K.K. Electron Tube Center, 1993, 1-53.
- 5 Knoll F. Proceedings of the IEEE, March 1983, **71**: 320-323.
- 6 Zeng H N, Xu S B, Liu S T, *et al.* Acta Photonica Sinica, 2001, **30**: 1321-1324.
- 7 Baccaro S, Blazek K, de Notaristefani F, *et al.* Nucl Instrum Methods Phys Res A, 1995, **A361**: 209-215.
- 8 Kuraray's Scintillation Materials, Specifications manual. Japan: Kuraray Company Limited, 1995: 1-36.
- 9 Belcari N, Damiani C, Guerra A D, *et al.* Nucl Instrum Methods Phys Res A, 2001, **A461**: 413-415.
- 10 Zhu J, Cheng L, Wang Z M. Acta Photonica Sin, 2006, **35**: 1497-1500.
- 11 Zhu Jie, Ma Hongguang, Ma Wenyan, *et al.* Nucl Sci Tech, 2007, **18**: 302-306.